

3.3.3. *The MISC Instrument*

3.3.3.1. *Science Traceability*

The Mid-Infrared Transit Spectrometer (MISC) instrument will observe at the shortest wavelengths of any of the OST instruments, ranging from 2.8 to 20 microns, and is optimized for measurements of bio-signatures in the atmospheres of transiting exoplanets. The first science step in this OST science goal will be to use the entire mid-IR wavelength range of the MISC transit spectrometer to search for and find at least 10 exoplanets with surface temperatures suitable for liquid water. Step 2 will make deeper observations of these candidates at 2.8-10 μm to find at least four candidates with bio-indicator molecules (CO_2 , H_2O). Finally, these candidates will be observed for longer integration times over multiple transits to detect the presence of bio-signature molecules (CH_4 , O_3 , N_2O) to at least the 3.6σ level. This requires a capability to measure the transmission spectra sensitive to CH_4 (3.3, 7.6 μm), N_2O (4.6, 7.8 and 17 μm), O_3 (9.6 μm), H_2O (6.3 μm), and CO_2 (4.2 μm) in the wavelength range from 3.0 to 19 μm . The MISC provides the OST with the observational capabilities to achieve those science objectives. Table 3.3.3.1 summarizes the basic measurement capabilities of the MISC instrument.

(Include a figure showing MISC in the observatory?)

Table 3.3.3.1. The MISC instrument fact sheet (baseline)

Parameter	MISC Transit Spectrometer
Observing modes	[1] MISC Ultra Stable Spectroscopy
Spectral Range	2.8 – 20 μ m (TRA-S; 2.8-5.5 μ m, TRA-M; 5.5-11 μ m, TRA-L; 11-20 μ m)
Resolving power	R=50 – 100 in 2.8 – 5.5 μ m (TRA-S) R=50 – 100 in 5.5 – 11 μ m (TRA-M) R=165 – 295 in 11 –20 μ m (TRA-L)
Angular resolution	Cannot attain spatially resolved information within the field of view
Field of View	Determined by the field stop size 2."5 in radius (TRA-S) 2."5 in radius (TRA-M) 1."7 in radius (TRA-L)
Detectors	A 2kx2k HgCdTe detector array (30K) for TRA-S A 2kx2k HgCdTe detector array (30K) for TRA-M A 2kx2k Si:As detector array with a calibration source for TRA-L A 256x256 HgCdTe detector array (30K) for TRA wavefront sensor
Photometric Stability	2.78ppm at 3 μ m (R=50) 3.24ppm at 5 μ m (R=50) 3.70ppm at 8 μ m (R=50) 4.65ppm at 10 μ m (R=50) 7.14ppm at 14 μ m (R=50; Glasse model) 13.39ppm at 14 μ m (R=200; Glasse model) 7.73ppm at 14 μ m (R=50; Wright model, l=0deg) 16.42ppm at 14 μ m (R=200; Wright model, l=0deg) 11.51ppm at 20 μ m (R=50; Glasse model) 23.69ppm at 20 μ m (R=300; Glasse model) 14.40ppm at 20 μ m (R=50; Wright model, l=0deg) 34.74ppm at 20 μ m (R=300; Wright model, l=0deg) on timescales of hours to days assuming 85 transits for K~8mag M-type star
Sensitivity; SNR/sqrt(hr)	SNR/sqrt(hr) = 12952 at 3.3 μ m SNR/sqrt(hr) = 13339 at 4.2 μ m SNR/sqrt(hr) = 9726 at 5 μ m SNR/sqrt(hr) = 9873 at 6.3 μ m SNR/sqrt(hr) = 8552 at 7.6 μ m SNR/sqrt(hr) = 8373 at 8 μ m SNR/sqrt(hr) = 7084 at 9.6 μ m SNR/sqrt(hr) = 6948 at 10 μ m SNR/sqrt(hr) = 4570 at 14 μ m SNR/sqrt(hr) = 3064 at 20 μ m assuming a R=50 with a 10.8 K-mag star
Saturation limit	29.8Jy at 3.3 μ m 27.5Jy at 6.3 μ m 4.4Jy at 14 μ m calculated for the shortest readout time; assuming partial readout, 10 μ sec per pixel per read, two reads per pixel to sample up the ramp

3.3.3.2 Instrument Description

3.3.3.2.1 General instrument operation principle

The Mid-infrared Spectrometer and Camera (MISC) transit spectrometer (TRA) is primarily dedicated to pointed observations to detect bio-signatures in habitable worlds in both primary and secondary transits of exoplanets. No simultaneous operation between the MISC and other instruments is expected. MISC TRA has three channels (TRA-S, TRA-M and TRA-L). The same FOV is shared among the three channels by means of beam splitters and all the channels are operated simultaneously to cover the full spectral range from 2.8–20 μm at once. A Lyot-coronagraph-based wavefront sensor (WFS) located in the instrument fore-optics uses the light reflected by a field stop, which corresponds to 0.3% of the light from the target, to send fine pointing information to the tip-tilt mirror in the OST telescope. The WFS measures the long-term drift using the point source image formed on the focal plane through a Lyot stop and feeds this information back to the observatory to mitigate the long-term drift down to 2 mas over a timescale of a few hours.

3.3.3.2.2 Overview of the MISC Instrument

The MISC transit spectrometer (MISC TRA) provides the highest ever spectro-photometric stability for 2.8–20 μm . A densified pupil spectroscopy is a newly-studied method for transit spectroscopy (Matsuo et al. 2016; Matsuo et al. 2018). This method will greatly improve spectro-photometric accuracy performance against optical disturbances. The science image is not disturbed by minor telescope pointing jitter (e.g., 9mas) or modest deformation of the telescope mirrors. A large number of science pixels minimizes intra- and inter-pixel sensitivity variations. A number of reference pixels are also employed for calibration of potential detector gain fluctuations with a cold photon shield mask. The block diagram of MISC TRA is shown in Figure 3.3.3.1. An optimal calibration technique using the reference pixels will be developed using a test bed of a prototype system during development. The MISC TRA will enable the detection of bio-signatures (e.g., ozone, water, and methane) in habitable worlds in both primary and secondary transits of exoplanets and makes the OST a powerful tool to bring a revolutionary progress in exoplanet sciences.

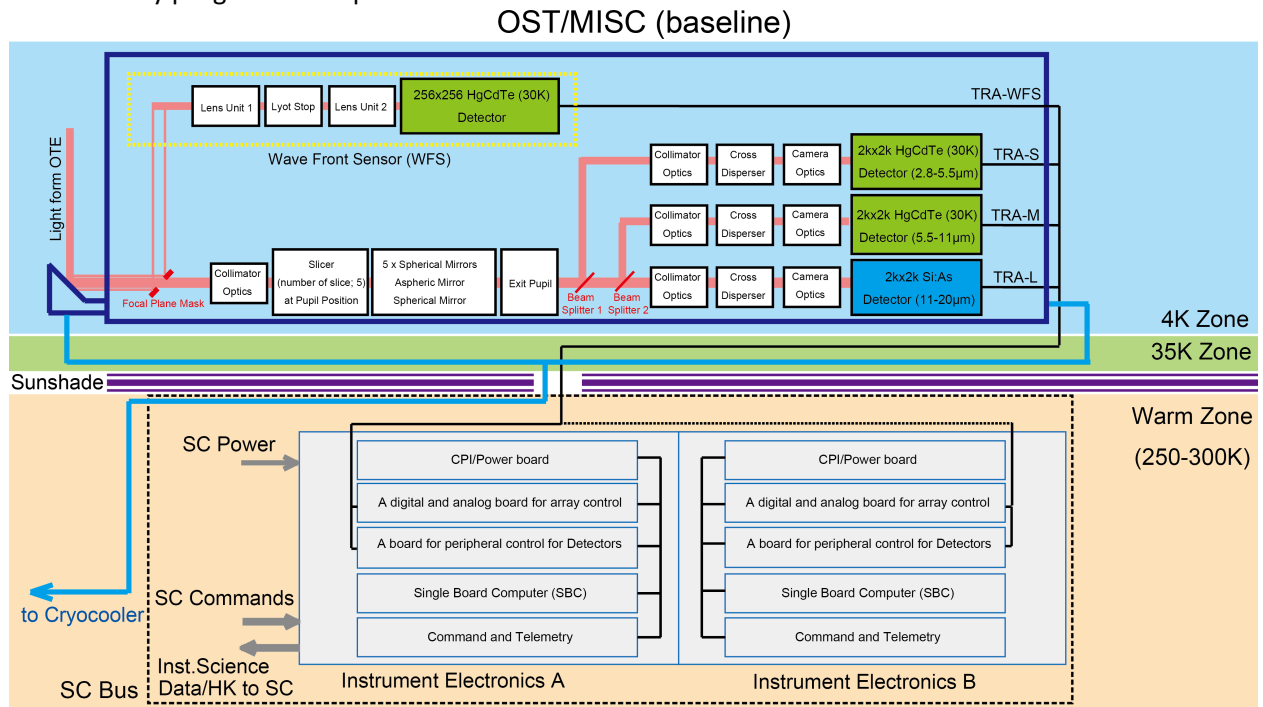


Figure 3.3.3.1. The block diagram of the MISC TRA

3.3.3.2.3 Optical design

The MISC TRA is designed based on the densified pupil spectroscopy (Matsuo et al. 2016). Unlike a conventional spectrograph, which performs spectroscopy in the focal plane, the densified pupil spectrograph carries out the spectroscopy in the pupil plane. The densified pupil spectrograph is composed of a pupil division/densification system followed by a normal spectrograph system (see Figure. 3.3.3.2). The pupil densification plays a key role in performing highly stable spectroscopy. Thanks to the pupil division (number of slices; 5) and the densification of the divided pupil, each of the densified sub-pupils acts as a point source and each corresponding beam is collimated by triple mirror assembly (TMA) collimator. The first dichroic beam splitter reflects the light of 11–20 μm , which is lead to the spectrograph of TRA-L, and transmits the light of <11 μm . The second dichroic beam splitter reflects the light of 5.5–11 μm , which is lead to the spectrograph of TRA-M, and transmits the light of <5.5 μm , which is lead to the spectrograph of TRA-S. Field stops with radii of 2."5, 2."5 and 1."7 are installed in the spectrograph TRA-S, TRA-M and TRA-L channels, respectively, to reduce the zodiacal background photons. We note that the aperture size of the field stop determines the size of field-of-view and no spatially resolved information within the field of view is obtained. A transmission grating (grism) is employed in each spectrograph to disperse the light in one dimension as a function of the wavelength on a detector plane. Each of the five spectra shares 271 pixels in the dispersion direction by 27 pixels in the cross dispersion direction for the TRA-S, 551 pixels in the dispersion direction by 54 pixels in the cross dispersion direction for the TRA-M, and 1586 pixels in the dispersion direction by 65 pixels in the cross dispersion direction for the TRA-L. The linear dispersion ($\Delta\lambda$) is set to 0.054 μm , 0.108 μm and 0.074 μm for TRA-S, TRA-M and TRA-L, respectively.

The MISC TRA is equipped with wave front sensor for the purpose of correcting any long-term drift in the telescope pointing. For this purpose, a trade study between a Lyot-Coronagraph-based wave front sensor and a guider camera with a dichroic beam splitter to extract 2-2.8 μm light of the target has shown a clear advantage in the Lyot-Coronagraph method in terms of the optical throughput of the MISC TRA, as well as in simplicity and cost. Figure 3.3.3.3 shows the schematic view of the MISC TRA wavefront sensor (WFS). The WFS uses only 0.3% of the light from the target host star, which is reflected by the focal plane mask in the fore-optics, and the majority (~98%) of the light from the target passes through $\phi 5''$ aperture in the focal plane mask and is lead to the TRA-S/M/L spectrometer channels. The long-term drift is measured by examining the position of the PSF centroid of the image produced on the detector plane of the WFS through the Lyot stop. Assuming that the actual Lyot stop size be produced as the same size of the OST pupil with an accuracy of 1%, the WFS will works for targets of M-type stars brighter than K=10mag. The WFS feeds back this information to the observatory and the long-term drift can be mitigated down to 2mas for M-type star brighter than K=10mag.

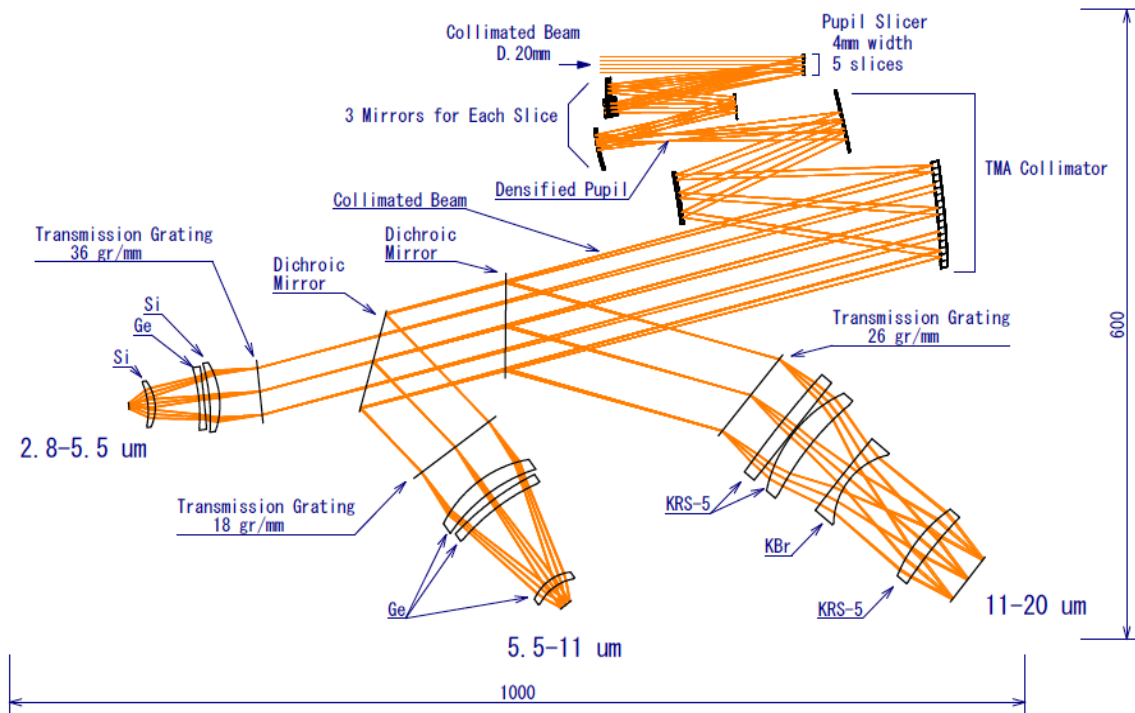


Figure 3.3.3.2. The result of the optical design of the MISC TRA (TB Updated with WFS?)

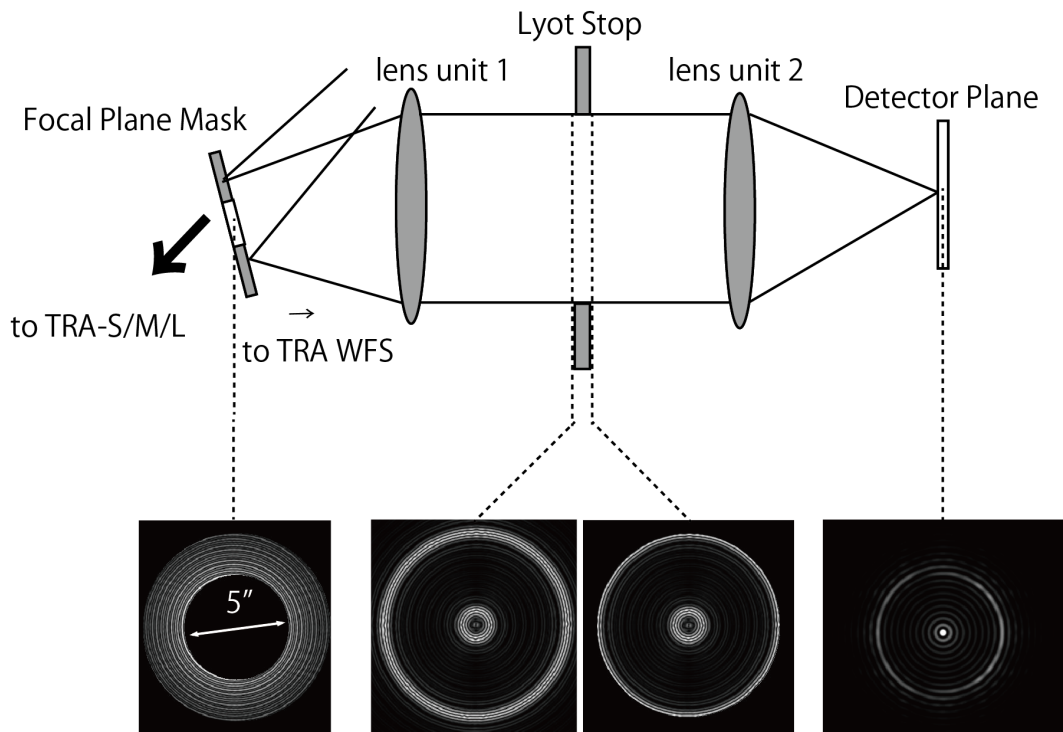


Figure 3.3.3.3. The schematic view of the MISC TRA WFS. The results of the simulation of PSF image at the focal plane mask, just before the Lyot stop, just after the Lyot stop, and the detector plate are shown.

3.3.3.2.4 Detection subsystem (or Focal plane(s), or Receiver Front End)

The MISC transit spectrometer employs two types of detectors: (1) HgCdTe that is bonded to a Si readout multiplexer and (2) Si Blocked Impurity Band (BIB) design that is bonded to a Si readout multiplexer. Each of the MISC TRA-S and TRA-M optical paths contains a 2k x 2k HgCdTe detector array operated at 30K and the MISC TRA wavefront sensor employs a 256 x 256 HgCdTe detector array operated at ~30K. HgCdTe detectors developed for the NEOCam mission have successfully demonstrated performance out to 10 μm (Dorn et al. JATIS 2016). The MISC TRA-L optical path contains a 2k x 2k Si:As detector array bonded to a Si readout multiplexer operating at ~8k to provide good detective quantum efficiency over the 10.5-20 μm wavelength range. Internal calibration sources are also employed to help achieve the required detector stability.

3.3.3.2.5 Signal amplification

Amplification of the signals from the detectors is a straightforward reuse of the technology used in previous space applications of Si:As BIB detectors such as Spitzer, JWST, and WISE, and will employ dedicated satellite chips that are located in close proximity to the detectors and also operate at cryogenic temperatures. HgCdTe detectors are used extensively in JWST and NEOCam and their readout designs can also be used with the MISC detectors.

3.3.3.2.6 Read-out electronics

Again, the readout electronics design of the MISC detectors is very similar to that used in previous space missions, and will incorporate flexible readout patterns and a variety of readout strategies, including double-correlated and Fowler sampling techniques.

3.3.3.2.7 Mechanical design

Based on the latest results of the mechanical design of the MISC, a 3D solid model of the MISC instrument is shown in Figure 3.3.3.4. In order to reduce the mass of the MISC instrument, we assume Be as a baseline material for the mirrors and mirror support structures as well as the base plate.

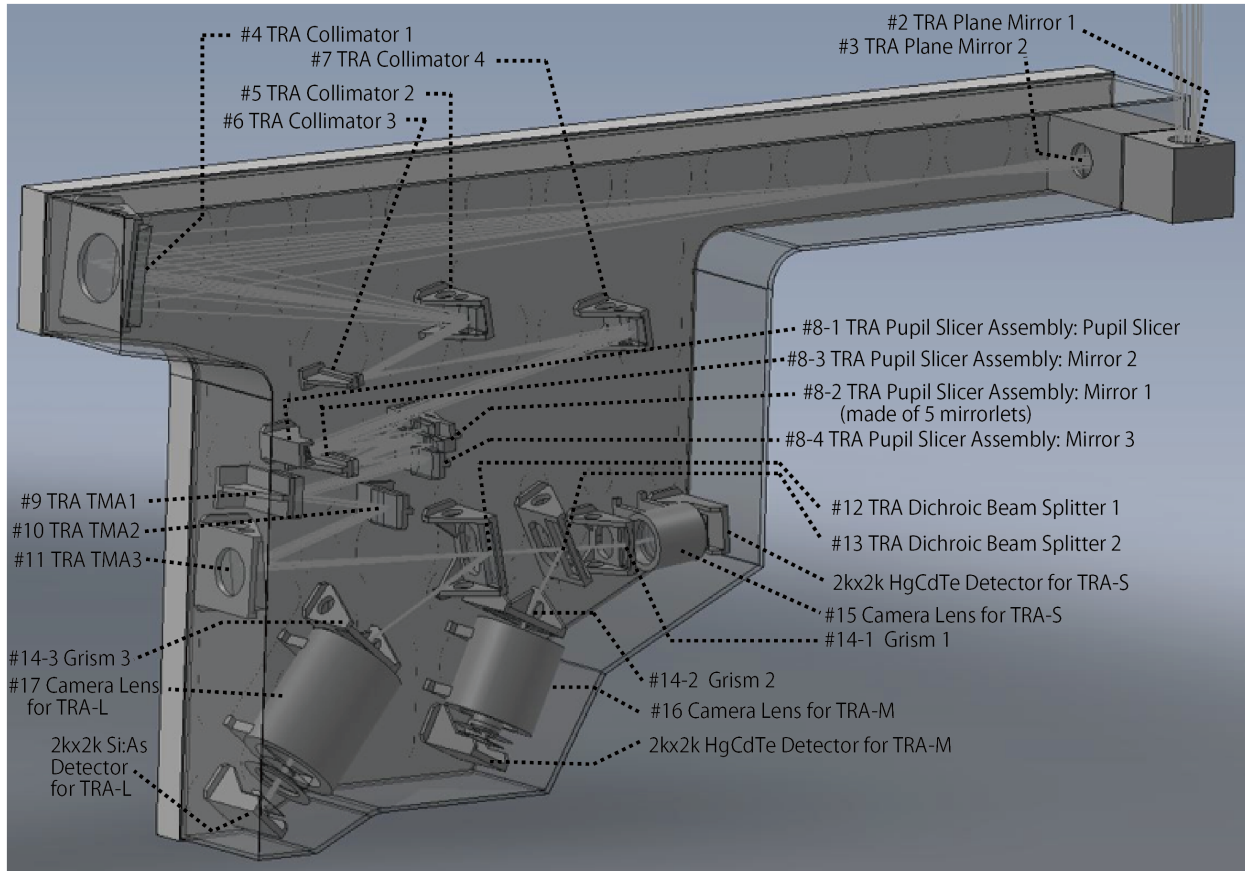


Figure 3.3.3.4. A 3D solid model of the MISC instrument. (TB Updated with WF guider?)

3.3.3.2.8 Mechanisms

The MISC TRA does not have any moving parts or mechanisms.

3.3.3.2.9. Instrument control

Each module has redundant dual-string warm electronics boxes (WEB A and WEB B for MISC TRA). Each electronics box contains a single board computer (SBC) and three boards; (i) a CPI/ Power board, (ii) a digital and analog board for array control (two 2kx2k HgCdTe arrays for TRA-S and TRA-M, one 2kx2k Si:As array for TRA-L, one 256x256 HgCdTe array for TRA WFS) and (iii) a board for peripheral control for detectors (two 2kx2k HgCdTe arrays for TRA-S and TRA-M, one 2kx2k Si:As array for TRA-L, one 256x256 HgCdTe array for TRA WFS). The SBC calculates the centroid position of the PSF on the WFS detector plate and send this information back to the observatory. The tip-tilt mirror in the observatory corrects for the pointing accuracy and mitigates the long-term drift down to a few mas over a timescale of a few hours.

3.3.3.2.10. Instrument Thermal architecture

The MISC instrument component will be located in two thermal zones. The Instrument optics and detectors will be located in a cold zone at the same $\sim 4.5\text{K}$ temperature as the telescope. The detectors themselves will have a weak thermal link to this cold temperature so that they can be heated slightly and held at a stable operating temperature. This operating temperature will be roughly 30K for the HgCdTe detectors and 8K for the Si:As detector. Baffling in the cold instrument will prevent IR light leakage from the warmer detectors reaching the Si:As detector. This can be successfully accomplished as demonstrated by the successful WISE mission which had both 32K detectors and 8K detectors located in the same instrument. The drive electronics that handle instrument data collection and communication with the spacecraft are all located in the $\sim 300\text{K}$ warm zone.

3.3.3.2.11. Contingency and margins

TBD

3.3.3.2.12. Instrument test facilities

The MISC instrument will require its own unique facilities for testing and calibration at the instrument level before it is delivered for integration with the observatory. Aside from the normal vibration, acoustic, and EMI environmental testing, the MISC instrument will need a thermal-vacuum test chamber that can be cooled to liquid helium temperatures that is large enough to enclose the complete cold section of the MISC instrument and is IR light-tight enough that stray light within the MISC detectors' sensitivity wavelengths is no greater than the infrared background what would be expected on-orbit. This test chamber should allow the introduction of IR signals at the expected levels of the on-orbit target sources and the ability to verify the spectral response of the spectrometer. Finally, the test facility will require an ultra-stable light source that can verify the \sim few ppm detector stability requirements needed for the exoplanet transit measurements. This test facility will need to allow connection between the cold MISC instrument assembly in the test chamber and the warm MISC drive electronics over flight-like cables.

The warm MISC instrument drive electronics will not require any particular test facilities other than the usual test facilities used to conduct vibration, acoustic, EMI, and thermal vacuum tests. A spacecraft simulator will be required to test command and data transfers between the MISC and spacecraft electronics.

3.3.3.2.13. Instrument Maturity

TBD

3.3.3.2.14. Observing modes and data rates

The MISC offers a single observing mode AOT01 (see Table 3.3.3.2). The MISC TRA-S, TRA-M and TRA-L share the same FOV by means of beam splitters and are simultaneously operated to produce 2.8–20 μ m spectra at once.

Table 3.3.3.2. The MISC observing modes (baseline)

AOT	Mode	Data rate
AOT01	MISC Transit Spectroscopy	1.59Mbps(max)—3.73Mbps(nominal) [MISC TRA] 0.37Mbps [MISC TRA WFS]

Note 1: Max data rate is calculated for the shortest exposure time $t_{exp}=4s$

Note 2: MISC TRA WFS assumes to read and down link 32 x 32 pixels around the PSF centroid at 20Hz

3.3.3.2.15. On-orbit checkout and calibration

In the beginning of the performance verification phase, the following items will be tested:

[PV-01] checkout of the condition of all boards in the warm electronics boxes

[PV-02] checkout of the condition of the detectors (e.g., clock patterns for all observing modes)

[PV-03] checkout of the condition of the internal calibration sources

[PV-04] checkout of the optical alignment

[PV-05] obtaining flat fielding images for each detector array

[PV-06] on-orbit absolute wavelength and flux calibration of the MISC TRA spectroscopic modes

During the nominal observational phase, the following calibrations are updated as needed:

[P1-01] dark current measurements (before and after each pointed observation)

[P1-02] annealing the detector arrays to remove hot pixels (beginning of every MISC obs. campaign)

[P1-03] checkout the stability of sensitivity by observing identical stars (once every few months)

We note that SOFIA and JWST may provide a new list of standard targets for flux/wavelength calibration. A stable internal calibration source is used to check the stability of the MISC TRA.

3.3.3.3 Risk management approach

As an instrument on a NASA Class A mission, the MISC instrument has a fully redundant, dual-string, cross-strapped design. The MISC instrument has a warm electronics box each with two redundant sets of warm electronics, as shown in the block diagram (Figure 3.3.3.1). Within an electronics box the single board computers and the rest of the warm electronics are cross-strapped as shown in Figure 3.3.3.5. Although the focal plane arrays are not dual redundant, their multiplexer readouts are arranged so that sections of the arrays fail gracefully as was done for the JWST instrument arrays.

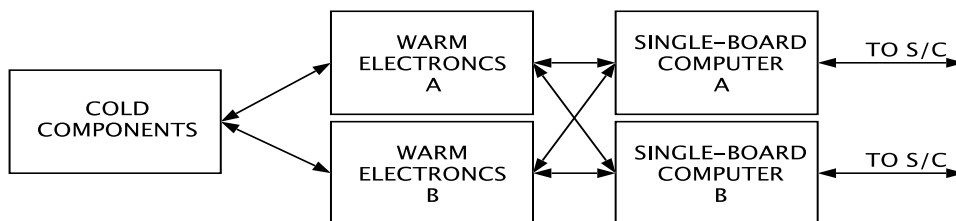


Figure 3.3.3.5 The cross-strapping design used in each of the MISC modules' warm electronics.

3.3.3.4 Resource requirements

Table 3.3.3.3 lists the resource requirements from the MISC on volume, mass, power and the data rates.

Table. 3.3.3.3 The resource requirements from the MISC instrument.

			MISC (baseline)		total
			MISC TRA	WFS	
Information related to the Electrical Subsystem	Total Max Data Rate	Mbps	1.49	0.37	1.86
	Total Average Data Rate	Mbps	3.73	0.37	4.10
Information related to the Mechanical model	Volume (cold component)	[m ³] (m x m x m)	0.15 (2.0 x 0.25 x 0.30) [foreoptics + wavefront sensor] 0.12 (1.0x 0.8 x 0.15) [Collimator + Pupil Mapping and Densification part + Spectrographs]		0.27
Information related to the Thermal Model	Mass (cold component)	[kg]	68.87		68.87
	Mass (warm component)	[kg]	16.00		16.00
	Mass (Others;e.g.,Harnessing)	[kg]	16.36		16.36
	Total Mass	[kg]	101.23		101.23
	Total Peak Power (cold part)	[W]	0.159	0.003	0.162
	Total Peak Power (warm part)	[W]	10	3	13
	Total Average Power (cold part)	[W]	0.009	0.003	0.012
	Total Average Power (warm part)	[W]	10	3	13
	Total Standby Power (cold part)	[W]	0.009	0.003	0.012
	Total Standby Power (warm part)	[W]	10	3	13
	Average Power Dissipation (detectors)	[W]	0.00804	0.00268	0.01072
	Average Power Dissipation (heater)	[W]	0.009	0.003	0.012

3.3.3.5 Predicted performance

The performance of the MISC TRA is calculated based on the following assumptions.

Throughput: The throughput curves as a function of the wavelength are calculated for TRA-S, TRA-M and TRA-L, taking account of the reflectance of mirrors (four mirrors for telescope optics, three mirrors for fore-optics, three collimator mirrors, seven mirrors in the densified pupil spectrograph), the transmittance/reflectance of the dichroic beam splitters, grating efficiency, transmittance of the AR-coated lenses, detector quantum efficiency and contamination/slit loss (see Figure 3.3.3.6).

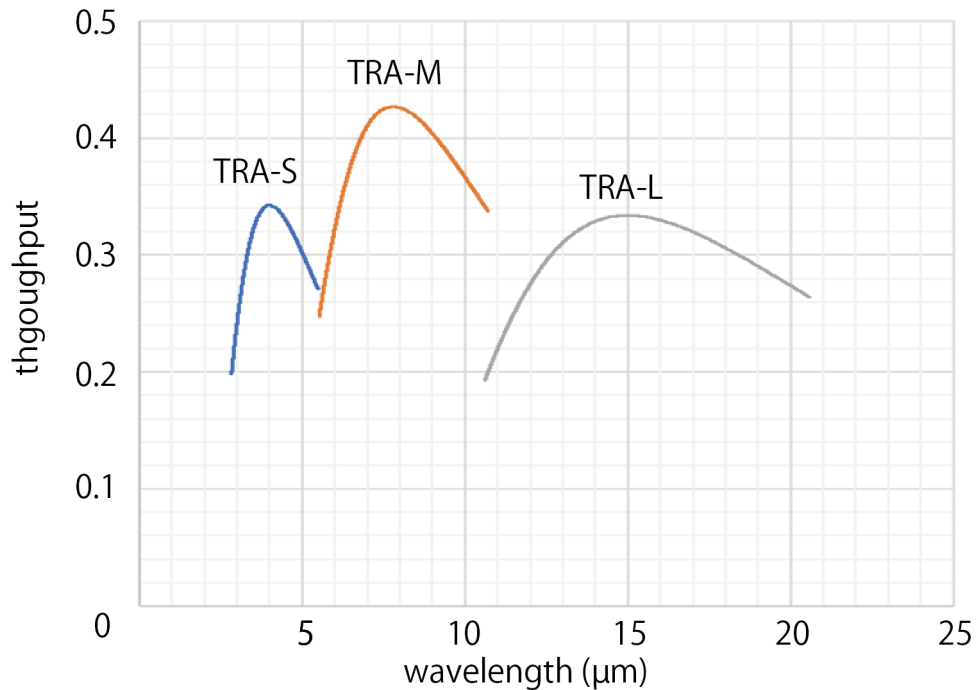


Figure 3.3.3.6 The throughput as a function of wavelength used for MISC TRA performance calculations.

Zodiacal light: The field of view of MISC TRA is determined by the size of the field stop (2."5 in radius for TRA-S and TRA-M, 1."7 in radius for TRA-L). The Glasse Zodiacal model (Glasse et al. 2015) is employed for the low background case outside the ecliptic plane while the Wright Zodiacal model for the ecliptic plane ($l=0$) (Wright et al. 1998) is employed for the high background case. The surface brightness of the zodiacal light including both scattered light and emissive components at representative wavelengths are summarized in Table 3.3.3.4.

Table. 3.3.3.4 The surface brightness of the zodiacal light used for MISC TRA performance calculations.

Wavelength (μm)	Low-background Case (MJy/sr) (Glasse model)	High-background Case (MJy/sr) (Wright model; at $l=0^\circ$)
3	0.1	
5	0.35	0.92
6	1	
8	3	
10	8.5	22.76
11	11	
14	14	46.58

Pointing jitter and long-term Drift: The major source of high-frequency pointing jitter is due to the cryocooler and is expected to be 9mas, RMS. A Lyot-Coronagraph-based wave front sensor (see section 3.3.3.2.3) is equipped to the MISC transit spectrometer and is used for measuring the long-term drift so that it can be compensated for by the tip-tilt mirror in the observatory. This mitigates the drift down to a few mas on a timescales of a few hours. Therefore, 4 mas is assumed for the drift over a timescale of a few hours.

Detector Performance: A 2k x 2k HgCdTe detector array operated at 30K is used in each of the MISC TRA-S and TRA-M channels and a 2k x 2k Si:As detector array operated at ~8K is used in MISC TRA-L. The detector dark current is assumed to be $1.0 \text{ e}^- \text{sec}^{-1} \text{pixel}^{-1}$ for the 2k x 2k HgCdTe detector and $0.2 \text{ e}^- \text{sec}^{-1} \text{pixel}^{-1}$ for the 2kx2k Si:As detector.

Based on the above assumptions, we have simulated the light curves of late-M type stars at different K-band magnitudes and calculated the spectrophotometric accuracy at representative wavelengths for each late-M type star. The results calculated for 84 transits and for a spectral resolution of $R=50$ are shown in Figures 3.3.3.7 – 3.3.3.14. The noise performances due to the photon noise, dark current, zodiacal light and jitter & drift are also indicated in each panel.

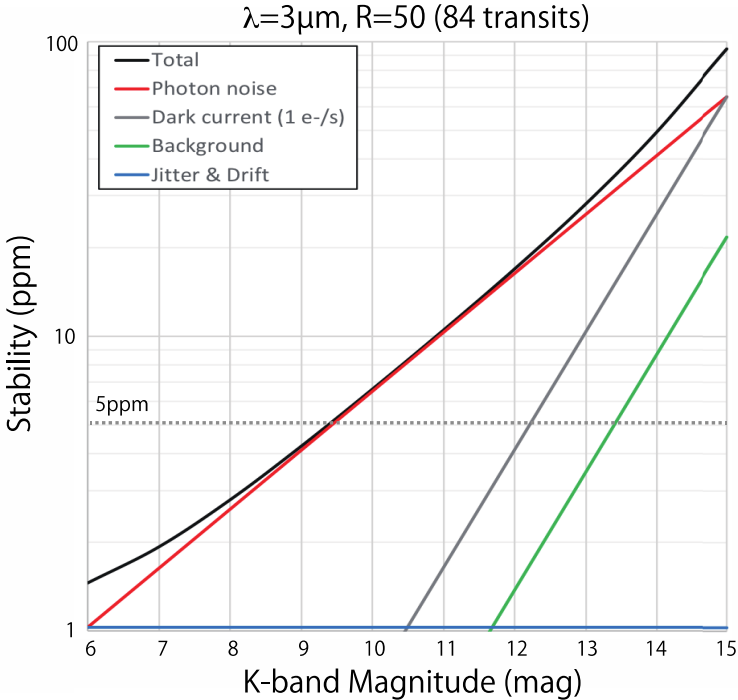


Figure 3.3.3.7 The spectro-photometric stability achieved by MISC TRA at $3\mu\text{m}$ with $R=50$.

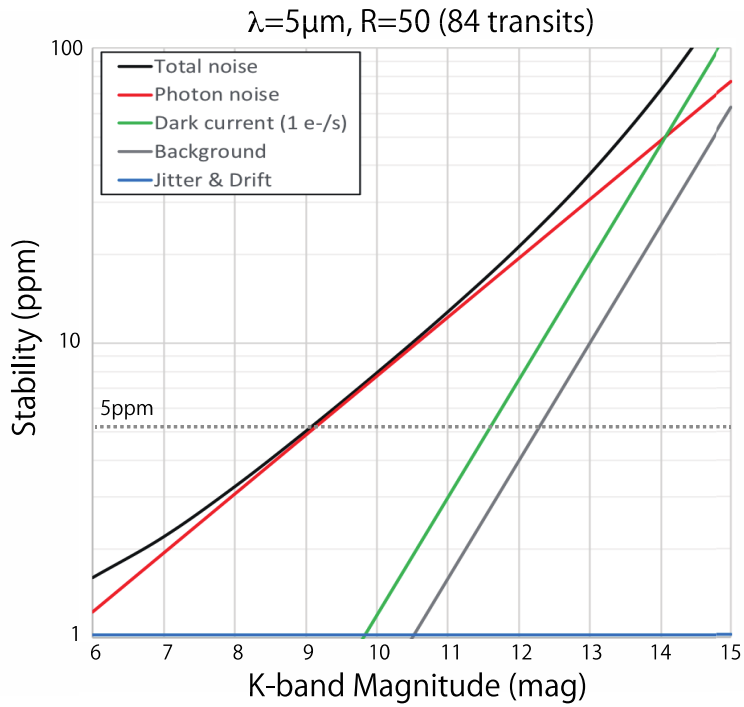


Figure 3.3.3.8 The spectro-photometric stability achieved by MISC TRA at $5\mu\text{m}$ with R=50.

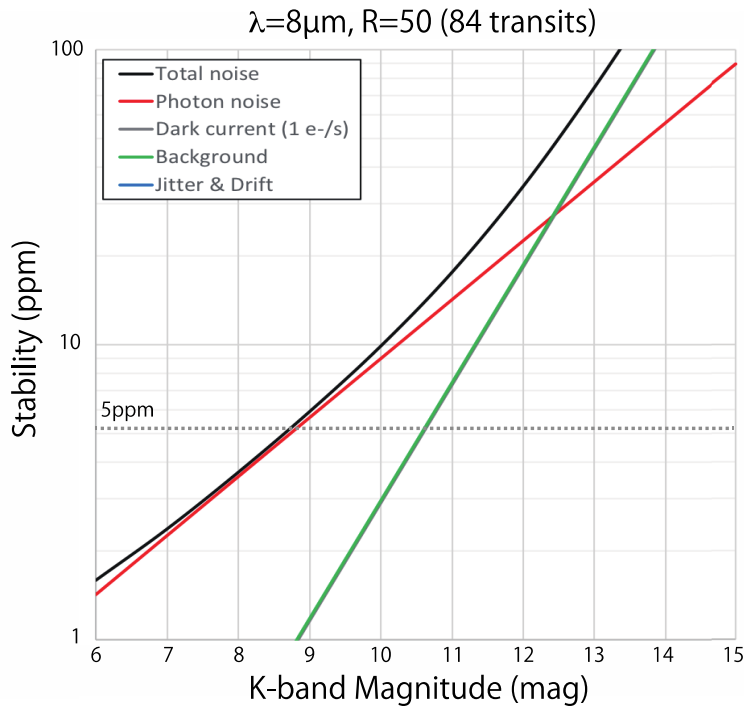


Figure 3.3.3.9 The spectro-photometric stability achieved by MISC TRA at $8\mu\text{m}$ with R=50.

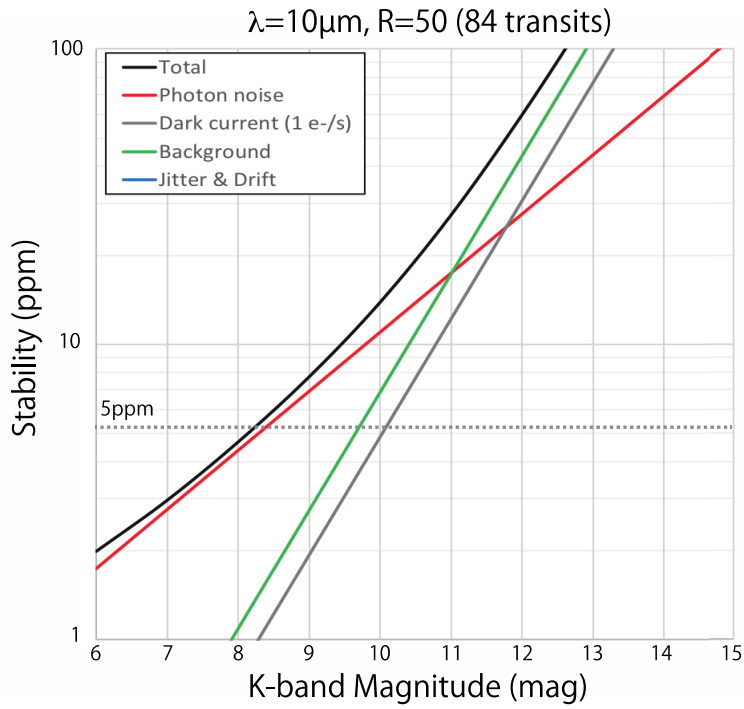


Figure 3.3.3.10 The spectro-photometric stability achieved by MISC TRA at $10\mu\text{m}$ with $R=50$.

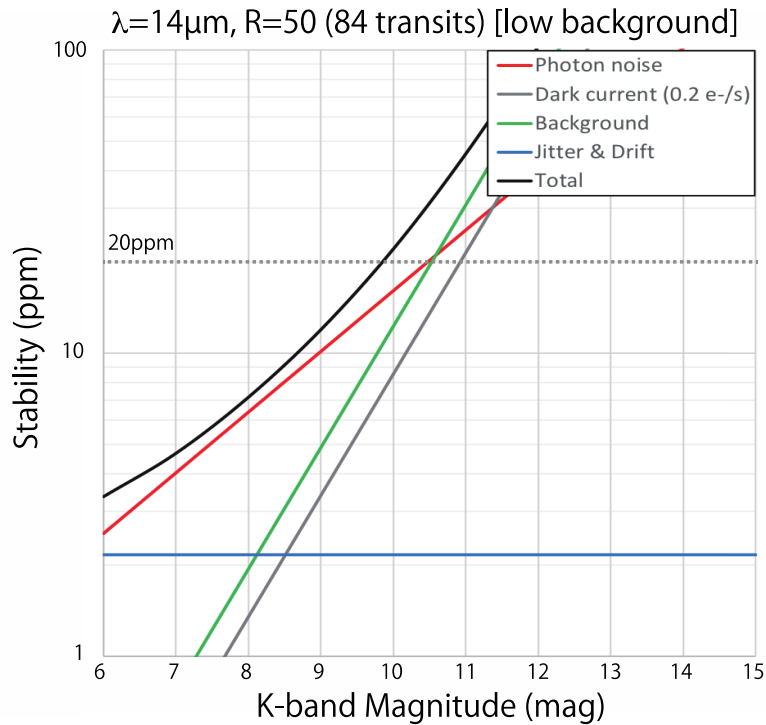


Figure 3.3.3.11 The spectro-photometric stability achieved by MISC TRA at $14\mu\text{m}$ with $R=50$ (low background case; Glasse et al. 2015).

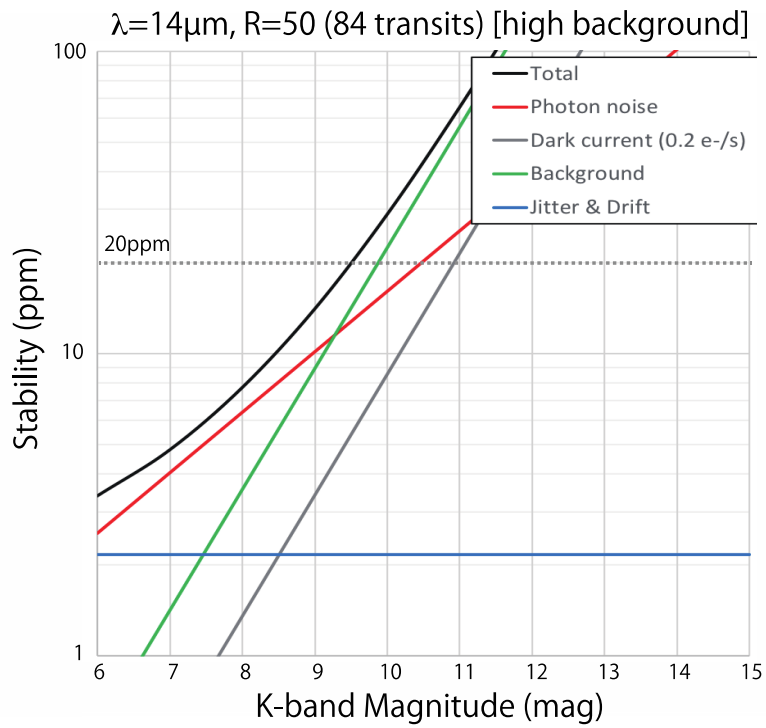


Figure 3.3.3.12 The spectro-photometric stability achieved by MISC TRA at $14\mu\text{m}$ with $R=50$ (high background case; Wright et al. 1998).

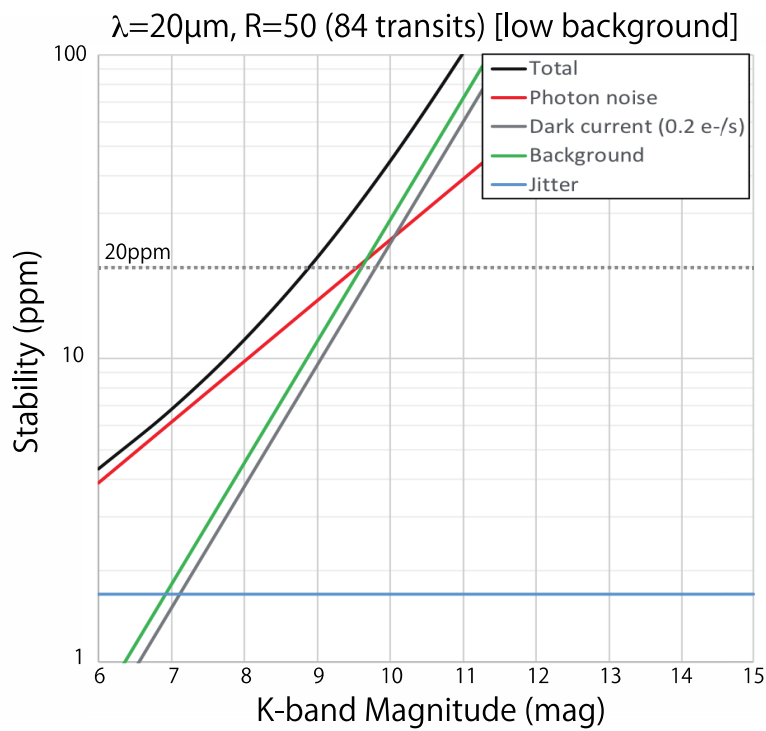


Figure 3.3.3.13 The spectro-photometric stability achieved by MISC TRA at $20\mu\text{m}$ with $R=50$ (low background case; Glasse et al. 2015).

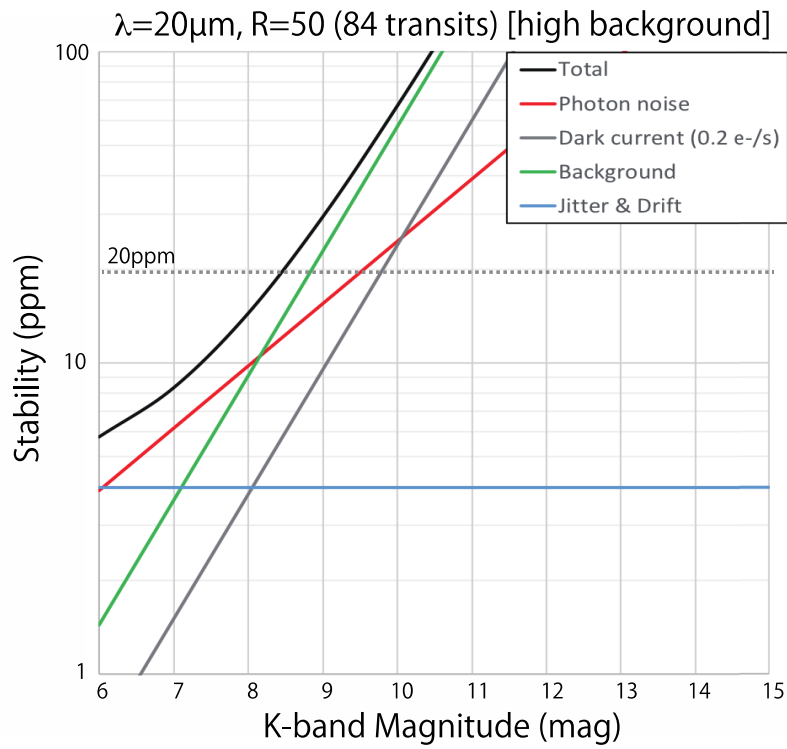


Figure 3.3.3.14 The spectro-photometric stability achieved by MISC TRA at $20\mu\text{m}$ with $R=50$ (high background case; Wright et al. 1998).

3.3.3.6 Alignment, Integration and Test

It will be necessary to develop specialized test hardware, but although the cope of this development will be significant it will be straightforward with no new technology development required. The integration and test of the MISC instrument is expected to take 12 months, assuming that all the external test support hardware and software is ready in time by the start of testing.

3.3.3.7 Heritage

The wavelength coverage and the capabilities of the MISC instrument are partly overlapping with those of the JWST/MIRI, SOFIA/FORCAST, SOFIA/EXES, SPICA/MCS, SPICA/SCI, SPICA/SMI, TAO/MIMIZUKU, Spitzer IRS, and TMT/MICHI instruments. How this heritage is employed within the different MISC components is shown in Table 3.3.3.5 below.

3.3.3.8 Enabling technology

Table 3.3.3.5 MISC Enabling Technology and Component Heritage

<i>Description</i>	<i>Subsystem/ Component</i>	<i>TRL</i>	<i>Heritage</i>
<i>Densified pupil spectrometer</i>	<i>subsystem</i>	<i>3 (5 by 2022)</i>	<i>New technology (Matsuo et al. 2016)</i>
<i>Be Mirrors and structures (including base plate)</i>	<i>component</i>	<i>6</i>	<i>NIRCam instrument on JWST</i>
<i>2kx2k Si:As with a calibration source</i>	<i>component</i>	<i>5</i>	<i>JWST/MIRI, SPICA/SMI</i>
<i>2kx2k HgCdTe</i>	<i>component</i>	<i>6</i>	<i>NEOCam</i>
<i>Beam Splitter, Short-wave cut filters (multi-layer interference filters)</i>	<i>component</i>	<i>5</i>	<i>AKARI/IRC, SPICA/MCS</i>
<i>Lyot stop (for wavefront sensor)</i>	<i>component</i>	<i>5</i>	<i>SPICA/SCI and others</i>

3.3.3.9 *Desclope options*

TBD (reducing the number of channels from three to two?)

3.3.3.10 *Partnership opportunities*

Throughout the OST Mission Concept studies, JAXA is leading the study of the MISC instrument with NASA Ames Research Center (NASA/ARC). The MISC instrument team is developing a testbed for a prototype of the densified pupil spectrograph at NASA/ARC, hoping to achieve TRL=5 by 2022. Laboratoire d'Astrophysique de Marseille is making a contribution to the study of the MISC instrument from both science and technical aspects. Further international partnership makes it more efficient to use the heritages of space-qualified components in other space IR missions and is desirable to complete the technical challenges that have low TRL at present.

7.1.11 *Summary*

The Mid-Infrared Spectrometer and Camera (MISC) instrument will observe at the shortest wavelengths of any of the OST instruments, ranging from 2.8 to 20 μm and is optimized for measurements of bio-signatures in the atmospheres of transiting exoplanets. This wavelength range allows measurements of the surface temperatures of the exoplanets as well as detections of the bio-signature molecules O₃, CH₄, H₂O, CO₂, and N₂O at Earth-levels, should they exist in an exoplanet atmosphere. The MISC instrument has a densified pupil spectrometer design with $R \sim 50$ -100 for 2.8–11 μm and $R \sim 165$ -295 for 11–20 μm and is capable of exoplanet transit and emission spectroscopy with very high spectro-photometric stability from 2.8 to 20.0 μm . The Lyot-Coronagraph based wave front sensor in the MISC instrument is used to measure the long-term drift. Using this information, the tip-tilt mirror in the observatory corrects for the pointing accuracy and mitigates the long-term drift down to a few mas over a timescale of a few hours. With these capabilities, the MISC instrument makes the OST a powerful tool to bring revolutionary progress in exoplanet sciences.